Received: 12 September 2019 | Accepted: 23 October 2019 | Published: 6 November 2019
DOI:10.20870/oeno-one.2019.53.4.2577

OENO One
VINE AND WINE OPEN ACCESS JOURNAL

Prediction of anthocyanin concentrations during red wine fermentation: development of Fourier transform infrared spectroscopy partial least squares models

Clément Miramont[1,2,3], Michael. Jourdes[1,2], Torben Selberg[3], Henrik Vilstrup Juhl[3], Lars Nørgaard[3] and Pierre-Louis Teissedre[1,2*]

[1]UR Œnologie EA 4577, Université de Bordeaux, ISVV, F-33140 Villenave d'Ornon, France
[2]USC 1366 Inra, IPB, Inra, ISVV, F-33140 Villenave d'Ornon, France
[3]FOSS Analytical A/S, DK-3400 Hillerød, Denmark

*Corresponding author: pierre-louis.teissedre@u-bordeaux.fr

ABSTRACT

Aim: The aim of the present study was to use Fourier transform infrared (FT–IR) spectroscopy with chemometrics to develop partial least squares (PLS) models to predict the concentrations of various anthocyanins during red wine fermentation.

Methods and results: Must and wine samples were collected during fermentation. To maximize diversity, 12 different fermentations, of two different vintages and two different varieties, were followed. The anthocyanin composition of the samples was characterized by using different reference analyses described in the literature: the concentration of free anthocyanins was determined by bisulphite bleaching, the concentration of molecular anthocyanins was determined by high-performance liquid chromatography with ultraviolet–visible detection, and the ratio of monomeric anthocyanins to polymeric anthocyanins was determined using the Adams–Harbertson assay. Finally, the data were analysed statistically by PLS regression to quantify laboratory-determined anthocyanin from FT–IR spectra. The correlations obtained showed good results for a large percentage of parameters studied, with the determination coefficient (R^2) for both calibration and cross-validation exceeding 0.8. The models for molecular anthocyanins appeared to overestimate their concentration, owing to intercorrelation with other parameters. Comparison of the data for each vintage indicated no apparent matrix effect per year, and data for other vintages should be compared to validate this hypothesis. The best models were those for monomeric or polymeric pigments and free anthocyanins.

Conclusions: By using FT–IR spectroscopy coupled with chemometrics, it is possible to create predictive models to estimate concentrations of anthocyanins and changes in global anthocyanin parameters during winemaking.

Significance and impact of the study: These results improve our understanding of anthocyanin prediction using FT–IR spectroscopy with chemometrics and pave the way for its use as a process control tool for the winemaker. They also highlight the propensity of chemometrics to overestimate certain predicted values when close parameters intercorrelate.

KEYWORDS

anthocyanins wine, FT-MIR Prediction, musts fermentation, chemometrics analysis

© 2019 International Viticulture and Enology Society - IVES

INTRODUCTION

Red wine is a beverage with one of the highest concentrations of phenolic compounds. These compounds are very rich in various metabolites and can be found in high quantities in grapes, at concentrations ranging from 2 to 11 g/kg (Singleton, 1966). One-third of these compounds are found in the skin and the other two-thirds in the seeds, with traces in the pulp and juice, depending on the grape variety (Zoecklein *et al.*, 2013). Extraction of phenolic compounds is highly dependent on the winemaking process. The total concentration of phenols in wine ranges between 1 and 5 g/L (Somers, 1971), rarely exceeding 50 % of their concentration in grapes.

Phenolic compounds have a major impact on wine quality. Polyphenols, particularly the flavonoids present in red wine, confer different chemical, qualitative and sensory characteristics. Anthocyanins are the second most important class of polyphenols in red grapes and are directly responsible for the colour of red wine, a major quality parameter for the consumer. The anthocyanins present and changes in anthocyanin composition over time are influenced by the wine matrix and parameters such as pH (Brouillard *et al.*, 1978; Forino *et al.*, 2019) and oxygen content (Iacobucci and Sweeny, 1983; Petrozziello *et al.*, 2018). These phenolic compounds are involved in pigment stability and oxygen consumption, and certain anthocyanin molecules can be used as markers (Avizcuri *et al.*, 2016). They can also reveal defects such as significant oxidation (Picariello *et al.*, 2017). Considering the potentially high impact of the anthocyanin composition of red wine, it is important to monitor the concentrations of anthocyanins during the different steps of winemaking and ageing.

Many methods have been developed to analyse anthocyanins in wine. However, most of them are time-consuming and require the use of chemistry skills and special equipment, making them unsuitable for rapid routine analysis. A reliable and rapid method to obtain measurements of anthocyanins is spectroscopy with chemometrics (Cozzolino *et al.*, 2004). The spectral regions for the quantification of red wine tannins have been investigated and identified, but interference resulting from the characteristic absorption bands of the major wine components precludes direct quantification (Jensen *et al.*, 2008). Chemometric treatment therefore appears to offer a solution by highlighting spectral information for use in building predictive models.

Fourier transform infrared (FT–IR) spectroscopy has already proved efficient in determining some of the main compounds in wine, such as ethanol, organic acids, phenols and sugars, and it is already being used as a cheap, rapid and efficient method of quantifying grape and wine compounds (Moreira and Santos, 2005; Bauer *et al.*, 2008; Pizarro *et al.*, 2011). Furthermore, recent studies have indicated the possibility of using FT–IR or ultraviolet–visible (UV/vis) spectroscopy with chemometrics to estimate concentrations of different polyphenolic compounds (Martelo-Vidal and Vázquez, 2014; Silva *et al.*, 2014; Rasines-Perea *et al.*, 2015; Aleixandre-Tudo *et al.*, 2018). However, some of these studies are limited by deficiencies in terms of number of samples analysed, diversity, and the use of grape fermentation techniques that reflect those used in non-research settings. Until now, some of the most comprehensive studies in which phenolic compounds have been measured have focused on must fermentations and the wines derived from them but not alcoholic fermentation specifically.

The aim of the present study was to develop an analytical application for winemakers, using a spectroscopic device to estimate anthocyanin content in must and wine during fermentation. Because the wine matrix has a major impact on the creation of predictive models (Wise and Gallagher, 1996; Geladi, 2003), this study focused on samples obtained during alcoholic fermentation and compared two different vintages to investigate how the wine matrix affects predictive models. Merlot and Cabernet Franc must and wine samples were collected during the 2017 and 2018 winemaking campaigns in Saint-Emilion, from harvest until run-off, and analytical methods (bisulphite bleaching; high-performance liquid chromatography, HPLC, with UV/vis detection; and the Adams–Harbertson assay) were carried out to quantify total, free and molecular anthocyanins and to determine the ratio of monomeric anthocyanins to polymeric anthocyanins. In parallel, the FT–IR spectra (925–5011 cm^{-1}) of the samples were registered, and the data obtained were analysed statistically using partial least squares (PLS) models to

 © 2019 International Viticulture and Enology Society - IVES

investigate correlations between the results of the anthocyanin analyses and the spectral data.

MATERIALS AND METHODS

1. Chemicals

Chemicals for the anthocyanin analyses, including bisulphite solution, tartaric acid, sodium hydroxide, sodium chloride, sodium metabisulphite, bovine serum albumin and malvidin-3-*O*-glucoside, were all analytical grade and purchased from Sigma-Aldrich (Saint Quentin Fallavier, France). Acids, including acetic acid, hydrochloric acid and formic acid, were all analytical grade and purchased from Fisher Scientific (Geel, Belgique). Solvents, including ethanol, methanol and acetonitrile, were all analytical grade and purchased from Prolabo-VWR (Fontenay-sous-Bois, France). Water was purified by a Milli-Q system (Millipore, Bedford, MA, USA).

2. Sample collection

All samples were collected during the 2017 and 2018 winemaking campaigns in Union de Producteurs de Saint-Emilion, Saint-Emilion, France. The contents of six fermentation tanks (four for Merlot and two for Cabernet Franc) were monitored each year, providing a total of 105 samples from 2017 and 60 samples from 2018. The contents of the tanks were intended to become commercial wines from the vineyards and were subject to real fermentation and winemaking conditions. The winemaking process was divided into three parts: prefermentation maceration for 4 days at 4 °C, alcoholic fermentation with commercial yeasts for 1 or 2 weeks, and post-fermentation maceration for 1–2 weeks until run-off.

The tanks were selected to provide variability in terms of grape variety, quality and soil. Approximately every 2 days from harvest until run-off, samples were collected from the tanks after pumping over to ensure homogeneity of their contents. Samples were sulphited at 2 g/hL and frozen at –23 °C. Before the anthocyanin analyses, samples were thawed then centrifuged at 4500 rpm to obtain supernatant; the temperature of the samples was then maintained at 4 °C during the analyses themselves. To avoid differences arising from differences in treatment of the samples, all were kept frozen for less than 3 months and the analyses were carried out in the 2 days after thawing.

3. Spectra measurement

All measurements were carried out in triplicate. Samples were scanned on a Winescan Flex (FOSS, Hillerød, Denmark) at a 3.858 cm^{-1} interval over the wavelength range 925–5011 cm^{-1}, with water as the reference blank. The spectra were registered in transmittance and converted into absorbance values before the chemometric analysis.

4. Analysis of anthocyanin composition

All analyses were carried out in triplicate.

4.1. Quantification of free anthocyanins by bisulphite bleaching

In this analysis, the concentration of free anthocyanins in the different samples was estimated using a method based on the ability of bisulphite to bleach these compounds (Ribéreau-Gayon and Stonestreet, 1965). Two tubes were prepared, one containing 1 mL of wine solution (250 µL of wine, 250 µL of ethanol with 0.1 % HCl v/v, and 5 mL of water with 2 % HCl v/v) and 400 µL of water, and another containing wine solution and 400 µL of bisulphite solution (15 % bisulphite v/v in water). After 20 min, the difference in absorbance at 520 nm between the two tubes was recorded and free anthocyanin concentration, expressed as malvidin-3-*O*-glucoside equivalent, determined by reference to a calibration curve established by Ribéreau-Gayon and Stonestreet.

4.2. Determination of the ratio of monomeric to polymeric pigments based on the Adams–Harbertson assay

The method used in this analysis is based on anthocyanin metabisulphite bleaching and the ability of polymeric pigment to precipitate with protein (Harbertson *et al*., 2003). Wine was diluted in a wine model buffer containing 12 % ethanol v/v and 5 g/L tartaric acid, adjusted to pH 3.3 with NaOH. In a first 1.5-mL microfuge tube, 500 µL of diluted wine was mixed with 1 mL of acetic acid–NaCl buffer (200 mM acetic acid and 170 mM NaCl, adjusted to pH 4.9 with NaOH). The absorbance at 520 nm of 1 mL of the mixture was read (the A value), then 80 µL of a 0.36 M sodium metabisulphite solution was added. After 10 min, the absorbance at 520 nm was read again (the B value). In a second microfuge tube, 500 µL of diluted wine was mixed with 1 mL of acetic acid–NaCl buffer

© 2019 International Viticulture and Enology Society - IVES

containing bovine serum albumin at 1 g/L. After 20 min, the tube was centrifuged for 5 min at 13500 *g*. One mL of the supernatant was mixed with 80 µL of a 0.36 M sodium metabisulphite solution. After 10 min, the absorbance at 520 nm was read (the C value).

The absorbance due to monomeric pigments is calculated as Δ (A–B), the absorbance due to small polymeric pigments is C, and the absorbance due to large polymeric pigments is calculated as Δ (B–C). Another parameter was added: the total polymeric pigments, which is the sum of the small polymeric pigments and the large polymeric pigments.

4.3. Quantification of molecular anthocyanins by HPLC–UV/vis

Twelve molecular anthocyanins were identified and quantified by HPLC–UV/vis (delphinidin-3-*O*-glucoside, cyanidin-3-*O*-glucoside, petunidin-3-*O*-glucoside, peonidin-3-*O*-glucoside, malvidin-3-*O*-glucoside, delphinidin-3-*O*-glucoside acetyl, cyanidin-3-*O*-glucoside acetyl, petunidin-3-*O*-glucoside acetyl, peonidin-3-*O*-glucoside acetyl, malvidin-3-*O*-glucoside acetyl, peonidin-3-*O*-glucoside coumaroyl and malvidin-3-*O*-glucoside coumaroyl), using the method described by Chira in 2009 and Paissoni more recently (Chira, 2009; Paissoni *et al.*, 2018). HPLC–UV/vis coupled with mass spectroscopy was used to determine retention times for the 12 different anthocyanins.

Wine samples were injected directly after filtration (pore diameter, 0.45 µm). Analyses were carried out on an Accela HPLC system (Thermo Fisher Scientific, Waltham, MA, USA) with 520 nm for the UV/vis wavelength detection. The column was a reverse-phase Nucleosil C18 (250 mm ´ 4 mm, 5 µm) (Agilent, Santa Clara, CA, USA). The flow was set at 1 mL/min, and the injection volume was 20 µL at 15 °C. The solvents used were (A) water–formic acid (95/5, v/v), and (B) acetonitrile–formic acid (95/5, v/v), with a gradient programme summarized in Table 1.

4.4. Analysis of chemometric data

This was done using Matlab 2017 (MathWorks, Natick, MA, USA) coupled with PLS_Toolbox by Eigenvector (Manson, WA, USA). Before PLS regression was carried out, autoscale preprocessing was applied to the data set. Autoscale is a preprocessing method that first uses mean-centring, followed by division of each variable by the standard deviation (SD) of that variable. The automatic variable selection (VIP or sRatio) proposed by PLS_Toolbox was used to refine spectral wavelengths selected to build the PLS regression. After this pretreatment,

TABLE 1. High-performance liquid chromatography gradient programme used to separate anthocyanins

Time (min)	0	25	35	40	41	46
Solvent A (%)	90	65	0	0	90	90
Solvent B (%)	10	35	100	100	10	10

Area peaks were plotted on a calibration curve produced from data obtained with malvidin-3-*O*-glucoside, and the results expressed as malvidin-3-*O*-glucoside equivalents (Figure 1).

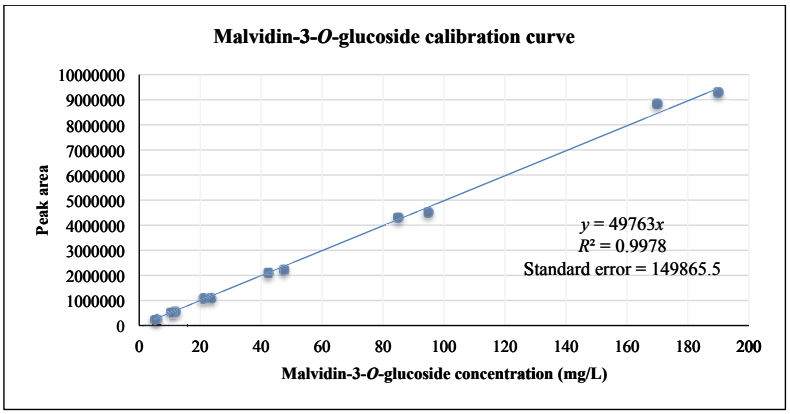


FIGURE 1. Malvidin-3-*O*-glucoside calibration curve for quantification of molecular anthocyanins by high-performance liquid chromatography with ultraviolet–visible detection

 © 2019 International Viticulture and Enology Society - IVES

calibration models were developed using PLS regression with leave-p-out cross-validation. Leave-p-out (with p equals 3) was set to avoid overestimation of results due to the triplicate process. A set of samples was removed from the data set and a PLS model built using the remaining data. The model obtained was applied to the removed set for evaluation, and this was repeated for every set.

For each model created, there were 10 cross-validation subgroups. The cross-validation result obtained is a good indicator of the model's ability to predict values for external samples. Moreover, to test the robustness of the models obtained using data for the samples from both vintages, the data were split into either a calibration set (66 %) or a validation set (33 %), using the Kennard–Stone algorithm (Kennard and Stone, 1969).

RESULTS AND DISCUSSION

1. References analysis

Regarding changes in the concentration of free anthocyanins during winemaking in 2017 and 2018 (Figure 2), the results indicate rapid extraction during the first week of alcoholic fermentation, followed by a steady decrease until run-off (Bautista-Ortín *et al.*, 2016). Anthocyanin extraction started the day after harvest, increased rapidly until reaching a peak, then slowly decreased. In both vintages, free anthocyanin concentration started between 50 and 300 mg/L on the first day in the tank after

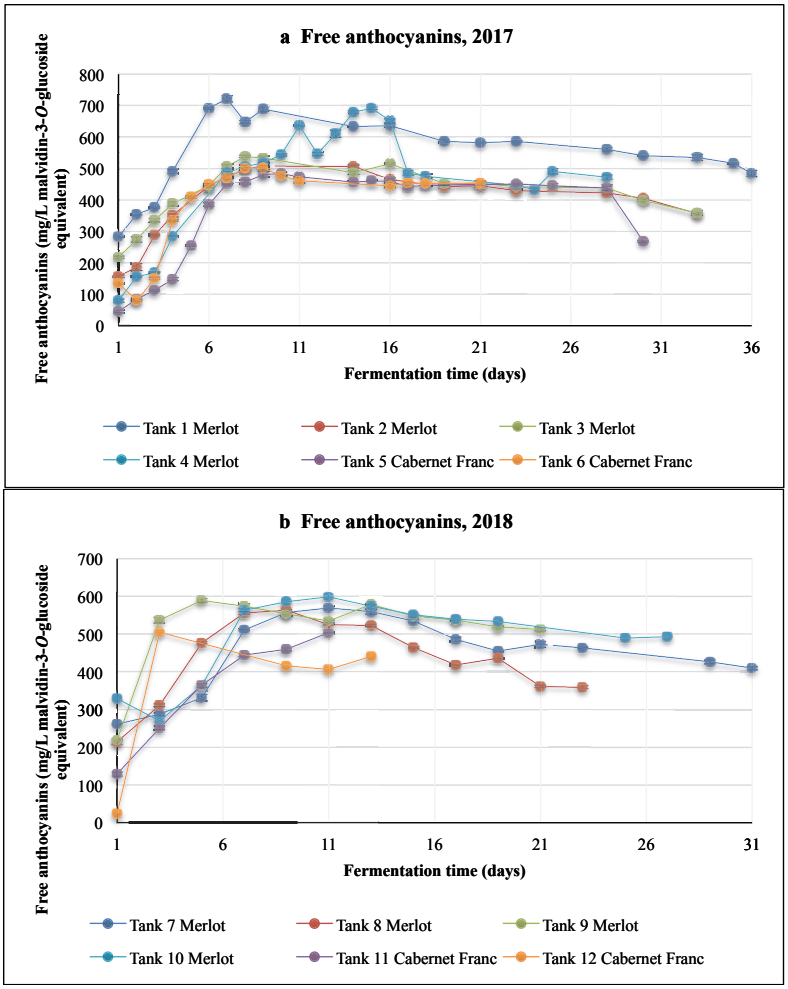


FIGURE 2. Quantification of free anthocyanins by bisulphite bleaching: results for 12 fermentation tanks
Free anthocyanins from the 2017 winemaking campaign in four different tanks of Merlot and two different tanks of Cabernet Franc.
Free anthocyanins from the 2017 winemaking campaign in four different tanks of Merlot and two different tanks of Cabernet Franc.

 © 2019 International Viticulture and Enology Society - IVES

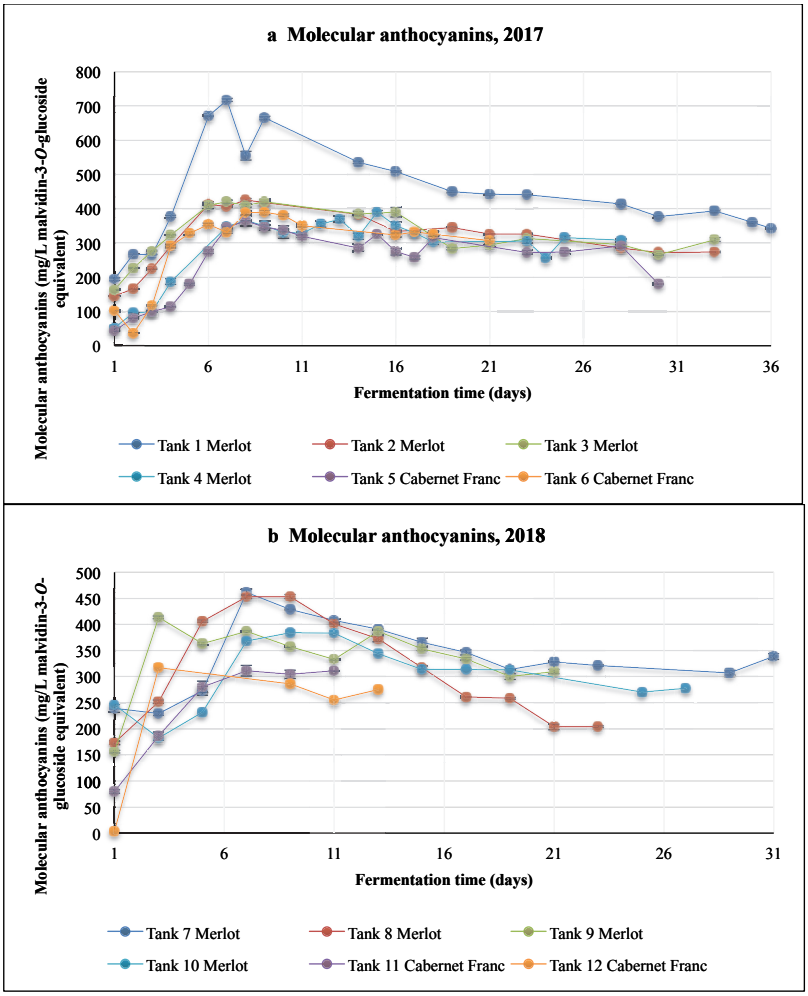


FIGURE 3. Quantification of molecular anthocyanins by high-performance liquid chromatography with ultraviolet–visible detection: results for 12 fermentation tanks.
Molecular anthocyanins from the 2017 winemaking campaign in four different tanks of Merlot and two different tanks of Cabernet Franc.
Molecular anthocyanins from the 2017 winemaking campaign in four different tanks of Merlot and two different tanks of Cabernet Franc.

harvest but increased rapidly to reach a maximum of between 400 and 700 mg/L in less than 10 days. Thereafter, a slow and constant decrease was observed until the last measurement during run-off (about 30 days after harvest), when the concentration was between 300 and 500 mg/L.

This trend was confirmed by the results of HPLC–UV/vis (Figure 3).

This specific pattern may be explained by the high extractability of anthocyanins in an aqueous solution, facilitated by the increasing volume of ethanol (Canals *et al.*, 2005). First, anthocyanin pigments are rapidly extracted from grape skins to reach a maximum. Once these compounds are in the wine matrix, they can interact and polymerize with flavan-3-ols to form oligomeric and polymeric pigments (Timberlake and Bridle, 1976; de Freitas and Mateus, 2010).

The Adams–Harbertson assay appears to be a good method for monitoring this polymerization. With relative absorbance determined for monomeric pigments, small polymeric pigments (procyanidins with fewer than four flavan-3-ol subunits that could not bind with bovine serum albumin) and large polymeric pigments, it is possible to monitor the ratios of these different pigments (Figure 4).

The Adams–Harbertson assay results clearly indicate changes in anthocyanin composition during winemaking and confirm polymerization over time as an explanation for the decrease in

 © 2019 International Viticulture and Enology Society - IVES

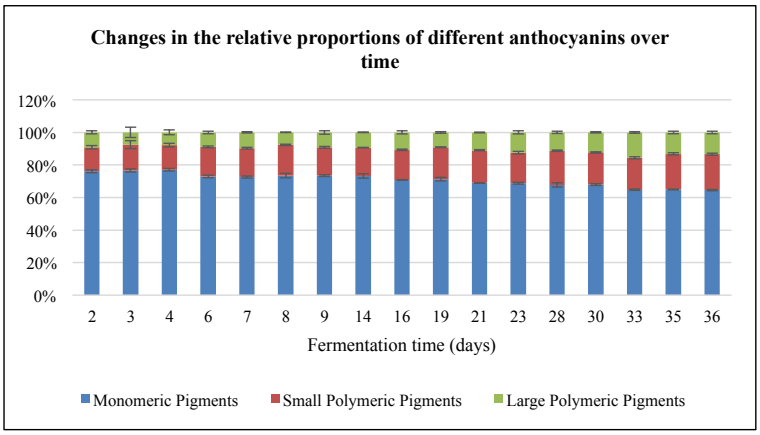


FIGURE 4. Changes in the ratio of different anthocyanin pigments (expressed as percentages of the total), over time: results for fermentation of Merlot, 2017, according to fermentation and post-fermentation days.

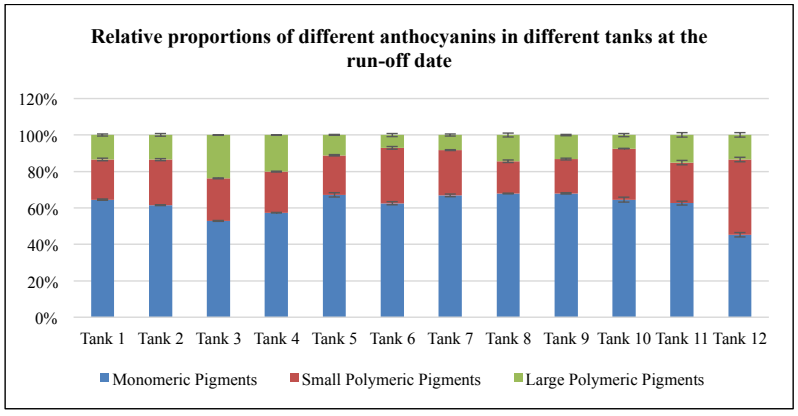


FIGURE 5. The ratio of different anthocyanin pigments (expressed as percentages of the total) in different tanks at the run-off date.

free anthocyanins shown by the results obtained by bisulphite bleaching and HPLC–UV/vis. The results for Merlot fermentation in 2017 indicate constant changes in the proportion of different pigments over time; there was a decrease in monomeric pigments from 76 % to 64 % in favour of polymeric pigments, with small polymeric pigments increasing from 4 % to 22 % and large polymeric pigments increasing from 9 % to 13 %.

The results for the end of fermentation, that is, at the run-off date (Figure 5), also show differences in anthocyanin composition between one fermentation and another, with samples from different tanks having slightly different proportions of the different kinds of pigment. For monomeric pigments, the mean was 62 % at the run-off date, with a maximum of 68 % and a minimum of 45 %. For small polymeric pigments, the mean was 25 % at the run-off date, with a maximum of 41 % and a minimum of 17 %. For large polymeric pigments, the mean was 13 % at the run-off date, with a maximum of 24 % and a minimum of 7 %.

Regarding anthocyanin concentrations during winemaking, rapid anthocyanin monitoring by FT–IR spectroscopy can be helpful for monitoring changes in these compounds over time. Moreover, variations in the ratio of monomeric to polymeric pigments appear to be linear during the fermentation and maceration process. A rapidly obtained FT–IR spectroscopy value can provide information on aspects of the winemaking process that can affect anthocyanin extraction and evolution, such as pumping over,

 © 2019 International Viticulture and Enology Society - IVES

addition of oenological tannins and micro-oxygenation.

2. Partial least squares regression models

Partial least squares regression models were built for each parameter studied for the 2017 vintage (Table 2), the 2018 vintage (Table 3), and the total for both years using data from all the samples (Table 4). To highlight the efficiency of the models and the variability of the parameters, we used the following: mean, SD, standard deviation of handling (SD handling), minimum (Min), maximum (Max), coefficient of variation (CV), coefficient of determination for calibration (R^2 cal), coefficient of determination for cross-validation (R^2 CV), coefficient of determination for prediction (R^2 pred), root mean square error of calibration (RMSE cal), root mean square error of cross-validation (RMSE CV), root mean square error of prediction (RMSE pred), relative percentage difference of cross-validation (RPD CV) and relative percentage difference of prediction (RPD pred).

The results indicate that anthocyanin concentrations were slightly higher for the 2018 vintage than for the 2017 vintage, with a mean total anthocyanin concentration determined by HPLC–UV/vis of 3079 mg/L for 2018 versus 2456 mg/L for 2017. However, variability was greater for the 2017 vintage, with an SD and a CV higher than those for the 2018 vintage. Regarding total anthocyanin concentration determined by HPLC–UV/vis, the SD and CV were 938 mg/L and 37.6 %, respectively, for the 2017 vintage, versus 873 mg/L and 28.5 %, respectively, for the 2018 vintage. The SD due to handling and instrument errors was always much lower than the SD of different parameters, showing that the variability was due mainly to variation in the studied parameter during fermentation and not to the SD handling.

3. Comparison of results for different vintages

Studying differences between the chemometrics results for each vintage and comparing them with the PLS models built using the total data set facilitates assessment of the importance of the wine matrix for each vintage and provides information on parameters that can influence the robustness of the models. If the addition of data from more samples generally helps increase the robustness of a model, a sizeable decrease in the predictivity of the total model compared with that of models for individual vintages could be the initial marker of incompatibility of prediction between vintages. Regarding the R^2 cal and the

TABLE 2. 2017 partial least squares regression results for anthocyanin parameters

Parameter	Mean	SD	SD handling	Min	Max	CV	R^2 cal	R^2 CV	RMSE C	RMSE CV	RPD CV
Delphinidin-3-*O*-glucoside (mg/L)	16.73	12.38	0.44	0.15	63.26	74.04	0.94	0.87	3.08	4.53	2.73
Cyanidin-3-*O*-glucoside (mg/L)	4.88	3.16	0.31	0.24	13.54	64.80	0.89	0.82	1.06	1.35	2.36
Petunidin-3-*O*-glucoside (mg/L)	19.67	12.46	1.12	0.12	74.71	63.36	0.90	0.79	4.03	5.91	2.16
Peonidin-3-*O*-glucoside (mg/L)	21.21	7.62	1.81	4.31	44.45	35.91	0.90	0.82	2.63	3.47	2.43
Malvidin-3-*O*-glucoside (mg/L)	106.79	38.40	2.72	14.32	229.34	35.96	0.92	0.90	10.85	12.42	3.09
Delphinidin-3-*O*-glucoside acetyl (mg/L)	5.89	2.78	0.38	0.26	12.97	47.17	0.94	0.90	0.69	0.89	3.14
Cyanidin-3-*O*-glucoside acetyl (mg/L)	2.71	1.18	0.24	0.14	5.14	43.39	0.89	0.84	0.39	0.48	2.49
Petunidin-3-*O*-glucoside acetyl (mg/L)	5.66	2.44	0.33	0.07	11.77	43.05	0.94	0.91	0.61	0.72	3.39
Peonidin-3-*O*-glucoside acetyl (mg/L)	6.91	2.67	0.36	1.29	11.88	38.69	0.90	0.83	0.85	1.13	2.39
Malvidin-3-*O*-glucoside acetyl (mg/L)	36.49	13.29	1.01	5.02	63.50	36.43	0.95	0.89	3.00	4.47	2.97
Peonidin-3-*O*-glucoside coumaroyl (mg/L)	3.70	1.75	0.20	0.17	7.98	47.38	0.93	0.87	0.47	0.64	2.73
Malvidin-3-*O*-glucoside coumaroyl (mg/L)	15.21	6.59	0.51	0.63	32.46	43.33	0.93	0.90	1.70	2.09	3.16
Total glucoside (mg/L)	169.27	68.99	4.57	20.55	411.77	40.75	0.93	0.91	17.78	20.93	3.29
Total acetyl (mg/L)	57.67	20.94	1.67	6.81	104.09	36.31	0.95	0.89	4.58	6.82	3.07
Total coumaroyl (mg/L)	18.91	8.27	0.64	0.80	40.31	43.72	0.96	0.91	1.76	2.52	3.28
Total anthocyanin (mg/L)	245.86	93.08	6.33	28.15	556.17	37.86	0.95	0.92	19.89	26.41	3.52
Free anthocyanin (mg/L)	432.85	147.04	8.97	44.86	721.20	33.97	0.95	0.90	34.29	45.89	3.20
Monomeric pigments (Abs*100)	12.66	5.47	0.30	1.10	23.19	43.19	0.96	0.91	1.11	1.62	3.37
Small polymeric pigments (Abs*100)	4.07	1.94	0.18	0.00	7.71	47.62	0.95	0.91	0.46	0.58	3.35
Large polymeric pigments (Abs*100)	1.69	1.49	0.27	0.00	7.52	87.73	0.89	0.68	0.49	0.87	1.72
Polymeric pigments (Abs*100)	5.77	3.03	0.17	0.49	14.90	52.60	0.95	0.90	0.66	0.95	3.20

 © 2019 International Viticulture and Enology Society - IVES

RMSE cal, both vintages showed good calibration (R^2 cal > 0.8), with slightly lower results for 2018. For this vintage, different molecular anthocyanin parameters had an R^2 cal under 0.8: malvidin-3-*O*-glucoside acetyl, cyanidin-3-*O*-glucoside acetyl, petunidin-3-*O*-glucoside acetyl and peonidin-3-*O*-glucoside acetyl. These specific anthocyanins were in very low concentrations in the wines studied, and lower variability and fewer samples for the 2017 vintage could explain the difficulty in correctly calibrating these compounds at lower concentrations. However, calibration results alone are not enough to evaluate the efficiency of a model and must be compared with cross-validation results to test the ability of a model to fit all samples in a calibration to the ability to predict values for external samples. Regarding the R^2 CV and the RMSE CV of the two vintages, the results followed the same tendency as for R^2 cal and RMSE cal. The results for the 2017 vintage indicate good cross-validation, with just one parameter (petunidin-3-*O*-glucoside) with an R^2 CV under 0.8. In contrast, in the results for the 2018 vintage, R^2 CV was above 0.8 for only five of the 21 parameters.

The last important parameter is the RPD CV, calculated using the following formula: SD/RMSE CV. According to the literature, an RPD under 1.4 indicates a non-reliable model for prediction; it must only be used as an indicator. If the RPD is greater than 1.4 and less than 2, the model starts being reliable enough to be used for prediction. If the RPD is above 2, the model starts to be considered good, and it is considered excellent if the RPD is above 3 (Cozzolino *et al.*, 2011; Ferrer-Gallego *et al.*, 2011; Martelo-Vidal and Vázquez, 2014). In the present study, only models with an RPD above 2 were considered sufficiently robust and predictive. Starting from this postulate, all parameters from the 2017 vintage can be accepted, except for large polymeric pigments. The lack of robustness and predictive power for this parameter can be easily explained by the very low concentration of large polymeric pigments determined during fermentation. Regarding the 2018 vintage, fewer than half the parameters can be considered good enough; the RPD results for this year are in many cases much lower than those for 2017. This may be due to a lack of variability and a lack of samples for the 2018 vintage compared with the 2017 vintage. The 2018 models are less able to correctly predict these parameters, owing to the complexity of extracting relevant information from the wine matrix. To highlight the

TABLE 3. 2018 partial least squares regression results for anthocyanin parameters

Parameter	Mean	SD	SD handling	Min	Max	CV	R^2 cal	R^2 CV	RMSE C	RMSE CV	RPD CV
Delphinidin-3-*O*-glucoside (mg/L)	21.32	9.26	0.75	0.17	42.00	43.43	0.90	0.56	2.94	6.69	1.38
Cyanidin-3-*O*-glucoside (mg/L)	4.45	2.97	0.36	0.06	11.34	66.82	0.89	0.63	0.98	1.91	1.56
Petunidin-3-*O*-glucoside (mg/L)	23.62	8.85	0.92	0.10	42.66	37.46	0.91	0.50	2.63	7.08	1.26
Peonidin-3-*O*-glucoside (mg/L)	23.26	10.64	0.97	0.53	49.51	45.75	0.89	0.62	3.51	6.89	1.55
Malvidin-3-*O*-glucoside (mg/L)	143.22	40.92	3.73	1.63	232.50	28.57	0.95	0.79	9.52	18.98	2.17
Delphinidin-3-*O*-glucoside acetyl (mg/L)	4.77	1.99	0.37	0.06	9.32	41.63	0.87	0.73	0.74	1.06	1.90
Cyanidin-3-*O*-glucoside acetyl (mg/L)	3.01	1.47	0.58	0.06	6.64	48.98	0.62	0.51	1.01	1.17	1.42
Petunidin-3-*O*-glucoside acetyl (mg/L)	5.82	2.21	0.64	0.06	10.14	38.01	0.70	0.62	1.28	1.43	1.62
Peonidin-3-*O*-glucoside acetyl (mg/L)	8.84	3.23	0.57	0.17	16.55	36.57	0.74	0.65	1.68	1.95	1.70
Malvidin-3-*O*-glucoside acetyl (mg/L)	44.77	14.55	1.87	0.53	76.97	32.50	0.79	0.74	6.73	7.51	1.96
Peonidin-3-*O*-glucoside coumaroyl (mg/L)	4.37	2.08	0.31	0.04	9.62	47.71	0.85	0.78	0.83	0.99	2.12
Malvidin-3-*O*-glucoside coumaroyl (mg/L)	19.85	8.48	0.91	0.07	36.68	42.74	0.95	0.90	1.87	2.62	3.27
Total glucoside (mg/L)	215.86	60.22	5.74	2.49	327.34	27.90	0.73	0.66	31.40	35.31	1.71
Total acetyl (mg/L)	67.21	19.64	3.02	0.88	105.64	29.22	0.84	0.73	8.03	10.47	1.90
Total coumaroyl (mg/L)	24.22	9.87	1.12	0.11	43.18	40.77	0.95	0.84	2.24	4.10	2.44
Total anthocyanin (mg/L)	307.29	87.43	9.09	3.49	461.68	28.45	0.82	0.69	37.59	49.64	1.77
Free anthocyanin (mg/L)	451.29	123.94	8.07	23.63	598.59	27.46	0.97	0.87	20.83	44.68	2.76
Monomeric pigments (Abs*100)	14.07	6.27	0.41	1.18	25.13	44.55	0.98	0.94	0.94	1.49	4.18
Small polymeric pigments (Abs*100)	4.69	2.06	0.28	0.00	10.70	43.94	0.93	0.76	0.54	1.02	2.03
Large polymeric pigments (Abs*100)	1.54	1.58	0.42	0.00	5.11	102.09	0.90	0.76	0.51	0.80	2.01
Polymeric pigments (Abs*100)	6.24	2.95	0.29	0.78	12.27	47.33	0.96	0.90	0.58	0.93	3.17

© 2019 International Viticulture and Enology Society - IVES

TABLE 4. Combined 2017 and 2018 partial least squares regression results for anthocyanin parameters

Parameter	Mean	SD	SD handling	Min	Max	CV	R^2 cal	R^2 CV	R^2 pred	RMSE C	RMSE CV	RMSE pred	RPD CV	RPD pred
Delphinidin-3-*O*-glucoside (mg/L)	18.40	11.53	0.55	0.15	63.26	62.69	0.90	0.83	0.78	3.71	4.77	5.29	2.42	2.18
Cyanidin-3-*O*-glucoside (mg/L)	4.72	3.09	0.32	0.06	13.54	65.47	0.85	0.79	0.77	1.21	1.45	1.44	2.15	2.16
Petunidin-3-*O*-glucoside (mg/L)	21.11	11.42	1.05	0.10	74.71	54.08	0.91	0.86	0.79	3.15	4.01	4.58	2.91	2.55
Peonidin-3-*O*-glucoside (mg/L)	21.96	8.86	1.51	0.53	49.51	40.36	0.86	0.77	0.71	3.46	4.42	4.74	2.12	1.97
Malvidin-3-*O*-glucoside (mg/L)	120.03	42.97	3.09	1.63	232.50	35.80	0.91	0.85	0.74	13.13	16.62	22.07	2.59	1.95
Delphinidin-3-*O*-glucoside acetyl (mg/L)	5.49	2.57	0.38	0.06	12.97	46.88	0.91	0.85	0.76	0.08	1.01	1.16	2.58	2.23
Cyanidin-3-*O*-glucoside acetyl (mg/L)	2.82	1.30	0.36	0.06	6.64	45.95	0.82	0.76	0.50	0.54	0.64	1.09	2.17	1.27
Petunidin-3-*O*-glucoside acetyl (mg/L)	5.72	2.35	0.44	0.06	11.77	41.13	0.87	0.78	0.69	0.88	1.14	1.26	2.11	1.91
Peonidin-3-*O*-glucoside acetyl (mg/L)	7.61	3.03	0.44	0.17	16.55	39.75	0.80	0.69	0.61	1.39	1.71	1.85	1.79	1.66
Malvidin-3-*O*-glucoside acetyl (mg/L)	39.50	14.29	1.33	0.53	76.97	36.17	0.92	0.85	0.73	4.06	5.62	7.83	2.55	1.84
Peonidin-3-*O*-glucoside coumaroyl (mg/L)	3.94	1.90	0.24	0.04	9.62	48.23	0.84	0.77	0.71	0.76	0.93	0.96	2.06	1.99
Malvidin-3-*O*-glucoside coumaroyl (mg/L)	16.90	7.64	0.66	0.07	36.68	45.24	0.91	0.84	0.78	2.35	3.06	3.63	2.52	2.12
Total glucoside (mg/L)	186.21	69.48	5.00	2.49	411.77	37.31	0.90	0.82	0.77	22.07	29.11	30.22	2.39	2.30
Total acetyl (mg/L)	61.14	20.93	2.16	0.88	105.64	34.23	0.90	0.76	0.67	6.65	10.43	10.61	2.02	1.98
Total coumaroyl (mg/L)	20.84	9.22	0.81	0.11	43.18	44.23	0.92	0.88	0.90	2.55	3.46	2.47	2.69	3.76
Total anthocyanin (mg/L)	268.19	95.51	7.33	3.49	556.17	35.61	0.91	0.86	0.82	29.38	36.16	33.91	2.65	2.83
Free anthocyanin (mg/L)	439.55	138.99	8.64	23.63	721.20	31.62	0.94	0.90	0.85	34.71	42.93	43.53	3.24	3.19
Monomeric pigments (Abs*100)	13.17	5.79	0.34	1.10	25.13	43.97	0.94	0.92	0.92	1.42	1.70	1.54	3.42	3.75
Small polymeric pigments (Abs*100)	4.30	2.00	0.22	0.00	10.70	46.56	0.90	0.84	0.73	0.65	0.82	0.93	2.46	2.15
Large polymeric pigments (Abs*100)	1.64	1.52	0.32	0.00	7.52	92.50	0.84	0.71	0.63	0.62	0.83	0.94	1.86	1.64
Polymeric pigments (Abs*100)	5.94	3.00	0.22	0.49	14.90	50.59	0.92	0.88	0.85	0.86	1.05	1.05	2.85	2.87

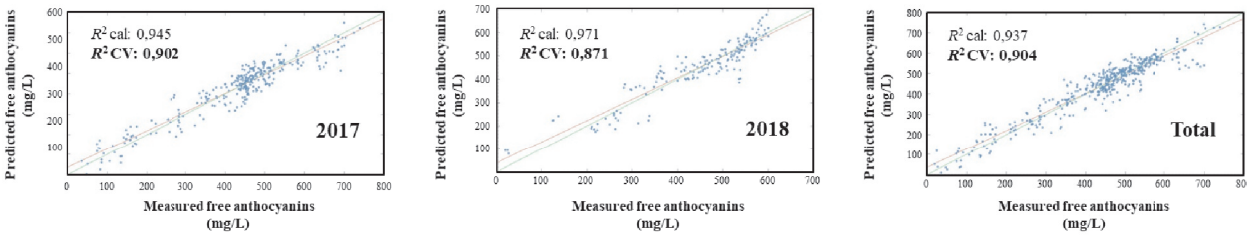


FIGURE 6. Partial least squares models for free anthocyanin parameters: comparison of results for 2017, 2018 and both years combined.

TABLE 5. Correlation between total anthocyanin and other molecular anthocyanin parameters

Parameter	Total anthocyanin (mg/L)
Delphinidin-3-*O*-glucoside (mg/L)	0.82
Cyanidin-3-*O*-glucoside (mg/L)	0.46
Petunidin-3-*O*-glucoside (mg/L)	0.89
Peonidin-3-*O*-glucoside (mg/L)	0.65
Malvidin-3-*O*-glucoside (mg/L)	0.97
Delphinidin-3-*O*-glucoside acetyl (mg/L)	0.76
Cyanidin-3-*O*-glucoside acetyl (mg/L)	0.68
Petunidin-3-*O*-glucoside acetyl (mg/L)	0.89
Peonidin-3-*O*-glucoside acetyl (mg/L)	0.76
Malvidin-3-*O*-glucoside acetyl (mg/L)	0.80
Peonidin-3-*O*-glucoside coumaroyl (mg/L)	0.85
Malvidin-3-*O*-glucoside coumaroyl (mg/L)	0.89
Total glucoside (mg/L)	0.98
Total acetyl (mg/L)	0.89
Total coumaroyl (mg/L)	0.92

possibility of a vintage effect, these results can be compared with the models built using data from all samples.

In the model parameters including data from all samples, the results show no decrease in robustness compared with the results for each of the two vintages taken separately. On the contrary, when most parameters have values between those of the two vintages, the model for free anthocyanins was more robust, due to the additive effect of the 2 years (Figure 6). Regarding R^2 CV, RMSE CV and RPD CV, which can be compared with the 2017 and 2018 models, the models for the totals for both years show similar results, with no apparent vintage effect. The fact that robustness does not decrease when data for the 2 years are combined is important for the development of chemometrics tools coupled with FT–IR spectroscopy. The models can therefore integrate other data to increase accuracy and robustness, and make this new tool more generic and able to predict anthocyanin concentrations in samples in a new winemaking campaign.

4. Results for the model combining data for both years

To further test the predictivity of the model, samples were separated into calibration and validation sets, and R^2 pred, RMSE pred and RPD pred were calculated. Regarding these values, the different parameters show high potential to be predictive using FT–IR spectroscopy.

Regarding the results for quantification of molecular anthocyanins by HPLC–UV/vis, many of the parameters have RPD pred above 2. They include delphinidin-3-*O*-glucoside,

 © 2019 International Viticulture and Enology Society - IVES

cyanidin-3-*O*-glucoside, petunidin-3-*O*-glucoside, delphini-din-3-*O*-glucoside acetyl, malvidin-3-*O*-glucoside coumaroyl, total glucoside, total coumaroyl and total anthocyanins. These results are in accordance with those of a study on fermenting samples and finished South African wines (Aleixandre-Tudo *et al*., 2018) and with other results for young wines (Romera-Fernández *et al.*, 2012). Regarding the all the parameters obtained, RPD tends to decrease with a low CV, but this tendency is not found for all molecular anthocyanin parameters. A question therefore arises: where does the robustness of these models come from? It can be difficult to achieve good prediction of values for specific molecules in low concentrations, such as molecular anthocyanins in a complex matrix. It is therefore possible that high predictivity is due to correlation with parameters other than the one targeted. Regarding changes in the concentration of anthocyanins during fermentation, the proportion of molecular anthocyanins stayed roughly the same during extraction (González-Neves *et al*., 2008), and except for the concentration of peonidin-3-*O*-glucoside, all molecular anthocyanin concentrations correlated well with total anthocyanin concentration (Table 5).

It may therefore be argued that the high predictivity of specific anthocyanins is due partly to an indirect correlation with total anthocyanins. This can be investigated using other varieties with different anthocyanin evolution, such as Pinot noir, which lacks acetylated anthocyanins (Dimitrovska *et al.*, 2011).

Quantification of free anthocyanin by bisulphite bleaching provides robust model parameters. All the RPD values were close to 3 and can be considered excellent models. Combination of data for the two vintages also increased robustness for this parameter compared with the results for a single vintage (Figure 6), showing that addition of data from other samples increases the predictivity of the model. The total results for cross-validation and prediction are close: RPD CV is 3.23 and RPD pred equal is 3.19. These high RPD values, and the similarity of these two results, confirm the robustness of the model and its ability to predict values for external samples.

Analysis of monomeric and polymeric pigments based on the Adams–Harbertson assay provided a ratio between monomeric and polymeric pigments, not a quantitative result. Therefore, it is not possible to consider the parameters separately; they must be considered as a set to express a ratio that can indicate anthocyanin evolution and polymerization during winemaking. RPD pred for monomeric anthocyanins, equal to 3.75 for the total data set, indicates a highly correlated and predictive model. RPD pred for small and large polymeric pigments was 2.15 and 1.64, respectively; both values are lower than the RPD pred for monomeric pigments. This marked decrease is easily explained by the very low concentration of polymeric pigments at the start of a wine's life. To increase the model's predictive power, the sample collection must include data from older wines with a higher concentration of polymeric pigments. Considering these results, polymeric pigments must not be broken down into small and large; only the distinction between monomeric and polymeric pigments should be made. RPD pred for polymeric pigments without distinction was 2.87 and expressed the same high predictivity as that for monomeric pigments. Therefore, it is possible to predict the evolution of anthocyanins during winemaking using FT–IR spectroscopy with chemometrics.

CONCLUSION

The results of the present study highlight the potential of rapid spectroscopic analysis to estimate the concentration and evolution of anthocyanins during winemaking. FT–IR spectroscopy combined with PLS regression provides a strong enough model for different anthocyanin parameters and is therefore able to provide winemakers with indications for choosing the appropriate process and conditions that can influence wine pigment concentration and quality. The apparent absence of a vintage effect in the two vintages studied indicates the possibility of making a prediction without systematically integrating samples from the current year. To validate this hypothesis, the models must be used to predict various vintages and the results compared with the results obtained using different methods described in the literature. To develop a reliable tool to assist winemakers, this study could now be complemented with studies using more samples from different varieties and regions, with the aim of enhancing variability. Regarding the results for molecular anthocyanins, varieties that

 © 2019 International Viticulture and Enology Society - IVES

express a different ratio of anthocyanins should be investigated. Nevertheless, some global models, such as free anthocyanins quantified by bisulphite bleaching, total anthocyanins quantified by HPLC–UV/vis, and the ratio of monomeric to polymeric pigments already show robust and predictive results with created models, which can now be tested in future winemaking campaigns to obtain full validation.

Acknowledgements: This study was financially supported by Innovation Found Denmark and FOSS Analytical A/S. All samples analysed were provided by Union de Producteurs de Saint-Emilion.

REFERENCES

Aleixandre-Tudo, J. L., Nieuwoudt, H., Aleixandre, J. L., & du Toit, W. (2018). Chemometric compositional analysis of phenolic compounds in fermenting samples and wines using different infrared spectroscopy techniques. *Talanta*, 176, 526-536. https://doi.org/10.1016/j.talanta.2017.08.065

Avizcuri, J. M., Sáenz-Navajas, M. P., Echávarri, J. F., Ferreira, V., & Fernández-Zurbano, P. (2016). Evaluation of the impact of initial red wine composition on changes in color and anthocyanin content during bottle storage. *Food chemistry*, 213, 123-134. https://doi.org/10.1016/j.foodchem.2016.06.050

Bautista-Ortín, A. B., Busse-Valverde, N., Fernández-Fernández, J. I., Gómez-Plaza, E., & Gil-Muñoz, R. (2016). The extraction kinetics of anthocyanins and proanthocyanidins from grape to wine in three different varieties. *OENO One*, 50(2). https://doi.org/10.20870/oeno-one.2016.50.2.781

Brouillard, R., Delaporte, B., & Dubois, J. E. (1978). Chemistry of anthocyanin pigments. 3. Relaxation amplitudes in pH-jump experiments. *Journal of the American Chemical Society*, 100(19), 6202-6205. https://doi.org/10.1021/ja00487a041

Canals, R., Llaudy, M. C., Valls, J., Canals, J. M., & Zamora, F. (2005). Influence of ethanol concentration on the extraction of color and phenolic compounds from the skin and seeds of Tempranillo grapes at different stages of ripening. *Journal of Agricultural and Food Chemistry*, 53(10), 4019-4025. https://doi.org/10.1021/jf047872v

Chira, K. (2009). *Structures moléculaire et perception tannique des raisins et des vins (Cabernet-Sauvignon, Merlot) du Bordelais* (Doctoral dissertation, Bordeaux 2).

Cozzolino, D., Kwiatkowski, M. J., Parker, M., Cynkar, W. U., Dambergs, R. G., Gishen, M., & Herderich, M. J. (2004). Prediction of phenolic compounds in red wine fermentations by visible and near infrared spectroscopy. *Analytica Chimica Acta*, 513(1), 73-80. https://doi.org/10.1016/j.aca.2003.08.066

Cozzolino, D., Cynkar, W. U., Shah, N., & Smith, P. (2011). Multivariate data analysis applied to spectroscopy: Potential application to juice and fruit quality. *Food Research International*, 44(7), 1888-1896. https://doi.org/10.1016/j.foodres.2011.01.041

Dimitrovska, M., Bocevska, M., Dimitrovski, D., & Murkovic, M. (2011). Anthocyanin composition of Vranec, Cabernet-Sauvignon, Merlot and Pinot noir grapes as indicator of their varietal differentiation. *European food research and technology*, 232(4), 591-600. https://doi.org/10.1007/s00217-011-1425-9

Ferrer-Gallego, R., Hernández-Hierro, J. M., Rivas-Gonzalo, J. C., & Escribano-Bailón, M. T. (2011). Determination of phenolic compounds of grape skins during ripening by NIR spectroscopy. *LWT-Food Science and Technology,* 44(4), 847-853. https://doi.org/10.1016/j.lwt.2010.12.001

Forino, M., Gambuti, A., Luciano, P., & Moio, L. (2019). Malvidin-3-O-glucoside Chemical Behavior in the Wine pH Range. *Journal of agricultural and food chemistry*, 67(4), 1222-1229. https://doi.org/10.1021/acs.jafc.8b05895

de Freitas, V. A., & Mateus, N. (2010). Updating wine pigments. *Recent advances in polyphenol research, Volume 2*, 59-80. https://doi.org/10.1002/9781444323375.ch3

Geladi, P. (2003). Chemometrics in spectroscopy. Part 1. Classical chemometrics. *Spectrochimica Acta Part B: Atomic Spectroscopy*, 58(5), 767-782. https://doi.org/10.1016/S0584-8547(03)00037-5

González-Neves, G., Gil, G., & Barreiro, L. (2008). Influence of grape variety on the extraction of anthocyanins during the fermentation on skins. *European Food Research and Technology*, 226(6), 1349. https://doi.org/10.1007/s00217-007-0664-2

Iacobucci, G. A., & Sweeny, J. G. (1983). The chemistry of anthocyanins, anthocyanidins and related flavylium salts. *Tetrahedron*, 39(19), 3005-3038. https://doi.org/10.1016/S0040-4020(01)91542-X

Jensen, J. S., Egebo, M., & Meyer, A. S. (2008). Identification of spectral regions for the quantification of red wine tannins with Fourier transform mid-infrared spectroscopy. *Journal of agricultural and food chemistry*, 56(10), 3493-3499. https://doi.org/ 10.1021/jf703573f

Kennard, R. W., & Stone, L. A. (1969). Computer aided design of experiments. *Technometrics*, 11(1), 137-148.

Martelo-Vidal, M. J., & Vázquez, M. (2014). Determination of polyphenolic compounds of red

 © 2019 International Viticulture and Enology Society - IVES

wines by UV–VIS–NIR spectroscopy and chemometrics tools. *Food chemistry*, 158, 28-34. https://doi.org/10.1080/00401706.1969.10490666

Moreira, J. L., & Santos, L. (2005). Analysis of organic acids in wines by Fourier-transform infrared spectroscopy. *Analytical and bioanalytical chemistry*, 382(2), 421-425. https://doi.org/10.1016/j.foodchem.2014.02.080

Paissoni, M. A., Waffo-Teguo, P., Ma, W., Jourdes, M., Rolle, L., & Teissedre, P. L. (2018). Chemical and sensorial investigation of in-mouth sensory properties of grape anthocyanins. *Scientific reports*, 8(1), 17098. https://doi.org/10.1038/s41598-018-35355-x

Petrozziello, M., Torchio, F., Piano, F., Giacosa, S., Ugliano, M., Bosso, A., & Rolle, L. (2018). Impact of Increasing Levels of Oxygen Consumption on the Evolution of Color, Phenolic, and Volatile Compounds of Nebbiolo Wines. *Frontiers in chemistry*, 6, 137. https://doi.org/10.3389/fchem.2018.00137

Picariello, L., Gambuti, A., Picariello, B., & Moio, L. (2017). Evolution of pigments, tannins and acetaldehyde during forced oxidation of red wine: Effect of tannins addition. *LWT*, 77, 370-375. https://doi.org/10.1016/j.lwt.2016.11.064

Pizarro, C., González-Sáiz, J. M., Esteban-Díez, I., & Orio, P. (2011). Prediction of total and volatile acidity in red wines by Fourier-transform mid-infrared spectroscopy and iterative predictor weighting. *Analytical and bioanalytical chemistry*, 399(6), 2061-2072. https://doi.org/10.1007/s00216-010-4356-6

Rasines-Perea, Z., Prieto-Perea, N., Romera-Fernández, M., Berrueta, L. A., & Gallo, B. (2015). Fast determination of anthocyanins in red grape musts by Fourier transform mid-infrared spectroscopy and partial least squares regression. *European Food Research and Technology*, 240(5), 897-908.

Ribéreau-Gayon, P., & Stonestreet, E. (1965). Determination of anthocyanins in red wine. *Bulletin de la Societe chimique de France*, 9, 2649. https://doi.org/10.1007/s00217-014-2394-6

Romera-Fernández, M., Berrueta, L. A., Garmón-Lobato, S., Gallo, B., Vicente, F., & Moreda, J. M. (2012). Feasibility study of FT-MIR spectroscopy and PLS-R for the fast determination of anthocyanins in wine. *Talanta*, 88, 303-310. https://doi.org/10.1016/j.talanta.2011.10.045

Silva, S. D., Feliciano, R. P., Boas, L. V., & Bronze, M. R. (2014). Application of FTIR-ATR to Moscatel dessert wines for prediction of total phenolic and flavonoid contents and antioxidant capacity. *Food chemistry*, 150, 489-493. https://doi.org/10.1016/j.foodchem.2013.11.028

Singleton, V. L. (1966). The total phenolic content of grape berries during the maturation of several varieties. *American Journal of Enology and Viticulture*, 17(2), 126-134.

Somers, T. C. (1971). The polymeric nature of wine pigments. *Phytochemistry*, 10(9), 2175-2186. https://doi.org/10.1016/S0031-9422(00)97215-7

Timberlake, C. F., & Bridle, P. (1976). Interactions between anthocyanins, phenolic compounds, and acetaldehyde and their significance in red wines. *American Journal of Enology and Viticulture*, 27(3), 97-105.

Wise, B. M., & Gallagher, N. B. (1996). The process chemometrics approach to process monitoring and fault detection. *Journal of Process Control*, 6(6), 329-348. https://doi.org/10.1016/0959-1524(96) 00009-1

Zoecklein, B., Fugelsang, K. C., Gump, B. H., & Nury, F. S. (2013). *Wine analysis and production*. Springer Science & Business Media.

 © 2019 International Viticulture and Enology Society - IVES